

# Vibration analysis of FG porous rectangular plates reinforced by graphene platelets

Changlin Zhou<sup>1</sup>, Zhongxian Zhang<sup>\*1</sup>, Ji Zhang<sup>1</sup>, Yuan Fang<sup>2</sup> and Vahid Tahouneh<sup>3\*\*</sup>

<sup>1</sup>School of Civil Engineering and Mechanics, Huazhong University of Science and Technology, Wuhan, Hubei, 430074, China

<sup>2</sup>General Construction Company of CCTEB Group Co., Wuhan, Hubei, 430064, China

<sup>3</sup>Young Researchers and Elite Club, Islamshahr Branch, Islamic Azad University, Islamshahr, Iran

(Received September 19, 2019, Revised December 1, 2019, Accepted December 2, 2019)

**Abstract.** The aim of this study is to investigate free vibration of functionally graded porous nanocomposite rectangular plates where the internal pores and graphene platelets (GPLs) are distributed in the matrix either uniformly or non-uniformly according to three different patterns. The elastic properties of the nanocomposite are obtained by employing Halpin-Tsai micromechanics model. The GPL-reinforced plate is modeled using a semi-analytic approach composed of generalized differential quadrature method (GDQM) and series solution adopted to solve the equations of motion. The proposed rectangular plates have two opposite edges simply supported, while all possible combinations of free, simply supported and clamped boundary conditions are applied to the other two edges. The 2-D differential quadrature method as an efficient and accurate numerical tool is used to discretize the governing equations and to implement the boundary conditions. The convergence of the method is demonstrated and to validate the results, comparisons are made between the present results and those reported by well-known references for special cases treated before, have confirmed accuracy and efficiency of the present approach. New results reveal the importance of porosity coefficient, porosity distribution, graphene platelets (GPLs) distribution, geometrical and boundary conditions on vibration behavior of porous nanocomposite plates. It is observed that the maximum vibration frequency obtained in the case of symmetric porosity and GPL distribution, while the minimum vibration frequency is obtained using uniform porosity distribution.

**Keywords:** porous nanocomposite plates; generalized differential quadrature method (GDQM); Halpin-Tsai micromechanics model; Vibration analysis

## 1. Introduction

Recently, Nanocomposites have significant importance for engineering applications that require high levels of structural performance and multi-functionality. Carbon nanotubes reinforced are at a research stage. However, there are several potential applications for these composites, such as Automobile and Aerospace industry, Space applications, Sports industry, Electronic packaging, sensors, Battery and energy storage. Carbon nanotubes have better strength and stiffness than carbon fibres and hence have the potential in replacing carbon fibre reinforced in various applications. These materials are considered as one of the most promising reinforcement materials for high performance structural and multifunctional composites with vast application potentials (Esawi and Farag 2007). A detailed summary of the mechanical properties of CNTs can be found in (Salvetat-Delmotte and Rubio 2002). The exceptional mechanical properties of CNTs have shown great promise for a wide variety of applications, such as

nanotransistors, nanofillers, semiconductors, hydrogen storage devices, structural materials, molecular sensors, field-emission-based displays, and fuel cells, to name just a few (Endo *et al.* 2004). The addition of nano-sized fibers or nanofillers, such as CNTs, can further increase the merits of polymer composites (Wernik and Meguid 2011). These nanocomposites, easily processed due to the small diameter of the CNTs, exhibit unique properties (Thostenson *et al.* 2001, Moniruzzaman and Winey 2006), such as enhanced modulus and tensile strength, high thermal stability and good environmental resistance. This behavior, combined with their low density makes them suitable for a broad range of technological sectors such as telecommunications, electronics (Valter *et al.* 2002) and transport industries, especially for aeronautic and aerospace applications where the reduction of weight is crucial in order to reduce the fuel consumption. For example, Qian *et al.* (2000) showed that the addition of 1 wt.% (i.e., 1% by weight) multiwall CNT to polystyrene resulted in 36-42% and ~25% increases in the elastic modulus and the break stress of the nanocomposite properties, respectively. In addition, Yokozeki *et al.* (2007) reported the retardation of the onset of matrix cracking in the composite laminates containing the cup-stacked CNTs compared to those without the cup-stacked CNTs. Most studies on CNT-reinforced composites (CNTRCs) have focused on their material properties (Hu *et*

\*Corresponding author, Ph.D.

E-mail: [zhxan1@163.com](mailto:zhxan1@163.com)

\*\*Ph.D.

E-mail: [vahid.tahouneh@ut.ac.ir](mailto:vahid.tahouneh@ut.ac.ir)

*al.* 2005, Fidelus *et al.* 2005, Bonnet *et al.* 2007, Hanand Elliott 2007, Odegard *et al.* 2003). Jin and Yuan (2003) determined the elasticity properties of single wall CNTs applying the molecular dynamic method. In fact, this macroscopic behavior was analyzed by studying the interaction of the atomic force and dynamic response in nanostructures affected by insignificant strain. Chang and Gao (2003) studied the dependence of single wall CNT elastic properties on its dimensions according to the molecular mechanics model. In fact, this model is one of the first studies for developing the analytical method application of molecular mechanic for modeling of nanostructures. Liu and Wang (2015) studied Thermal vibration of a single-walled carbon nanotube predicted by semiquantum molecular dynamics. Zhang and Wang (2018) investigated the nonlinear thermal vibrational behavior of single-layered BP (SLBP) via a nonlinear orthotropic plate model (OPM) and molecular dynamics (MD) simulations. Xu *et al.* (2016) studied the vibration of double-layered graphene sheets (DLGS) using A nonlocal Kirchhoff plate model with the van der Waals (vdW) interactions. The concept of FGM can be utilized for the management of a material's microstructure so that the vibrational behavior of a plate/shell structure made of such material can be improved. In recent years, two kinds of FGMs are designed to improve mechanical behavior of plate/shell structures. One is functionally graded fiber-reinforced composites that have a smooth variation of material volume fractions, and/or in-plane fiber orientations, through the radial direction. Another one is functionally graded metal/ceramic composites with continuous composition gradation from pure ceramic on one surface to full metal on the other (Matsunaga 2008). According to a comprehensive survey of literature, the authors found that there are few research studies on the mechanical behavior of functionally graded CNTRC structures. Shen (2009) for the first time suggested that the nonlinear bending behavior can be considerably improved through the use of a functionally graded distribution of CNTs in the matrix. He introduced the CNT efficiency parameter to account load transfer between the nanotube and polymeric phases. Compressive postbuckling and thermal buckling behavior of functionally graded nanocomposite plates reinforced by aligned, straight single-walled CNTs (SWCNTs) subjected to in-plane temperature variation were reported by Shen and Zhu (2010) and Shen and Zhang (2010). They found that in some cases the CNTRC plate with intermediate CNT volume fraction does not have intermediate buckling temperature and initial thermal postbuckling strength. Marin *et al.* (2013) proved the uniqueness theorem and some continuous dependence theorems without recourse to any energy conservation law, or to any boundedness assumptions on the thermoelastic coefficients using the Lagrange identity. Composites with microstructure display nonlocal effects and can be effectively modeled through dipolar elasticity. A mixed initial boundary problem was addressed for dipolar thermoelasticity by Marin and Craciun (2017). Marin *et al.* (2017) investigated the theory of micropolar thermoelastic bodies whose micro-particles possess microtemperatures. They transformed the mixed initial boundary value problem

into a temporally evolutionary equation on a Hilbert space and after that they proved the existence and uniqueness of the solution. Hassan *et al.* (2018) studied convective heat transfer performance and fluid flow characteristics of Cu-Ag/water hybrid nanofluids. Othman and Marin (2017) studied the wave propagation of generalized thermoelastic medium with voids under the effect of thermal loading due to laser pulse with energy dissipation. Matsunaga (2000) investigated a two-dimensional, higher-order theory for analyzing the thick simply supported rectangular plates resting on elastic foundations. Yas and Sobhani (2010) studied free vibration characteristics of rectangular continuous grading fiber reinforced (CGFR) plates resting on elastic foundations using DQM. Three dimensional vibration analysis of multi-layered graphene sheets embedded in polymer matrix was investigated by Alibeigloo (2013). Tahouneh *et al.* (2013) studied 3D free vibration analysis of continuous grading fiber reinforced annular plates via 2D DQ method. Arefi (2015) suggested an analytical solution of a curved beam with different shapes made of functionally graded materials (FGMs). Bennai *et al.* (2015) developed a new refined hyperbolic shear and normal deformation beam theory to study the free vibration and buckling of functionally graded (FG) sandwich beams under various boundary conditions. Bouchafa *et al.* (2015) used refined hyperbolic shear deformation theory (RHSDT) for the thermoelastic bending analysis of functionally graded sandwich plates. Barka *et al.* (2016) studied thermal post-buckling behavior of imperfect temperature-dependent FG structures. Chen *et al.* (2017) investigated vibration and stability of initially stressed sandwich plates with FGM face sheets. Bouguenina *et al.* (2015) studied FG plates with variable thickness subjected to thermal buckling. Wu and Liu (2016) developed a state space differential reproducing kernel (DRK) method in order to study 3D analysis of FG circular plates. Park *et al.* (2016) used modified couple stress based third-order shear deformation theory for dynamic analysis of sigmoid functionally graded materials (S-FGM) plates. Tahouneh (2016) presented a 3-D elasticity solution for free vibration analysis of continuously graded carbon nanotube-reinforced (CGCNTR) rectangular plates resting on two-parameter elastic foundations. The volume fractions of oriented, straight single-walled carbon nanotubes (SWCNTs) were assumed to be graded in the thickness direction. Moradi-Dastjerdi and Momeni-Khabisi (2016) studied Free and forced vibration of plates reinforced by wavy carbon nanotube (CNT). The plates were resting on Winkler-Pasternak elastic foundation and subjected to periodic or impact loading. Liew *et al.* (1996) employed the differential quadrature method for studying the Mindlin's plate on Winkler foundation. Cheng and Batra (2000) used Reddy's third-order plate theory to study steady state vibrations and buckling of a simply supported functionally gradient isotropic polygonal plate resting on a Pasternak elastic foundation and subjected to uniform in-plane hydrostatic loads. Ahmed Houari *et al.* (2018) presented a closed-form solutions for exact critical buckling loads of nonlocal strain gradient functionally graded beams. Tornabene *et al.* (2019) investigated free vibration analysis of arches and beams

made of composite materials via a higher-order mathematical formulation. Tornabene *et al.* (2017) studied free vibration analysis of composite sandwich plates and doubly curved shells with variable stiffness. The reinforcing fibers were located in the external skins of the sandwich structures according to curved paths. Tornabene *et al.* (2018) studied free vibration of laminated nanocomposite plates and shells using first-order shear deformation theory and the Generalized Differential Quadrature (GDQ) method. Each layer of the laminate was modelled as a three-phase composite. A survey of several methods under the heading of strong formulation finite element method (SFEM) was presented by Tornabene *et al.* (2015). Jabbari *et al.* (2013, 2014) examined porosity distribution effect on buckling characteristics of saturated porous plates. Chen *et al.* (2015) studied static bending and buckling of metal foam porous beams with functionally graded (FG) porosities using a shear deformation beam model.

In this research, free vibration analysis of metal foam plates reinforced with GPLs is carried out applying 3-D theory of elasticity model considering different porosity distributions. GPLs are distributed in the thickness direction with uniform and nonuniform models. Uniform, symmetric, and asymmetric distributions of porosity have been considered.

## 2. Problem description

Consider a rectangular plate with length  $a$ , width  $b$ , and thickness  $h$  as depicted in Fig. 1. The deformations defined with reference to a Cartesian coordinate system  $(x, y, z)$  are  $u, v$  and  $w$  in the  $x, y$  and  $z$  directions, respectively.

## 3. Porous GPL-reinforced plate model with different porosity distributions

The structure has continuous grading of GPLs-reinforcement through thickness direction. Three different GPL dispersion patterns, denoted by A, B, and C, are considered for each porosity distribution (Fig. 2). The GPL volume content  $V_{\text{GPL}}$  is assumed to vary along the  $z$ -axis smoothly with its peak values ( $S_{ij}$ ,  $i, j=1, 2, 3$ ) being determined based on the specific porosity distribution.

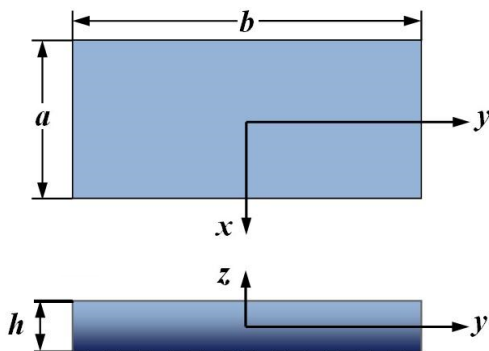


Fig. 1 The sketch of a thick nanocomposite rectangular plate and setup of the coordinate system

To facilitate a direct and meaningful comparison, the total amount of GPLs is kept the same for three different GPL distribution patterns. This leads to  $S_{i1} \neq S_{21} \neq S_{31}$  ( $i=1, 2, 3$ ). The mechanical properties of a porous plate with different types of porosity distributions can be expressed by

$$E(z) = E_1(1 - e_0 \lambda(z)) \quad (1)$$

$$G(z) = E(z) / 2(1 + \nu(z)) \quad (2)$$

$$\rho(z) = \rho_1(1 - e_m \lambda(z)) \quad (3)$$

in which, for symmetric porosity distribution

$$\lambda(z) = \cos(\pi z / h) \quad (4)$$

for asymmetric porosity distribution

$$\lambda(z) = \cos(\pi z / 2h + \pi / 4) \quad (5)$$

and for uniform porosity distribution

$$\lambda(z) = \lambda \quad (6)$$

where  $E_1$ ,  $G_1$ , and  $\rho_1$  are the maximum values of elasticity moduli, shear moduli and mass density.

Also,  $e_0$  and  $e_m$  are the coefficients of porosity and mass density, respectively, defined by (Kitipornchai *et al.* 2017)

$$\begin{aligned} e_0 &= 1 - \frac{E_2}{E_1} = 1 - \frac{G_2}{G_1} \\ e_m &= \frac{1.121(1 - 2\sqrt[3]{1 - e_0 \lambda(z)})}{\lambda(z)} \end{aligned} \quad (7)$$

Also based on the closed-cell grapheme-reinforcement scheme, Poisson's ratio ( $\nu$ ) can be expressed by (Kitipornchai *et al.* 2017)

$$\nu(z) = 0.221 \tilde{p} + \nu_1(0.342 \tilde{p}^2 - 1.21 \tilde{p} + 1) \quad (8)$$

In which  $\nu_1$  is the Poisson's ratio of pure matrix materials without pores and

$$\tilde{p} = 1.121(1 - 2\sqrt[3]{1 - e_0 \lambda(z)}) \quad (9)$$

Also,  $\lambda(z)$  for uniform porosity distribution can be expressed by

$$\lambda = \frac{1}{e_0} - \frac{1}{e_0} \left( \frac{\tilde{M}/h + 0.121}{1.121} \right)^{2.3} \quad (10)$$

In which

$$\tilde{M} = \int_{-h/2}^{h/2} (1 - \tilde{p}) dz \quad (11)$$

According to the distribution patterns depicted in Fig. 2, the volume fraction of GPLs can be written as ( $i=1, 2, 3$ )

$$V_{\text{GPL}} = \begin{cases} S_{i1} [1 - \cos(\pi z / h)], \text{ Pattern A} \\ S_{i2} [1 - \cos(\pi z / 2h + \pi / 4)], \text{ Pattern B} \\ S_{i3}, \text{ Pattern C} \end{cases} \quad (12)$$

The relation between the volume fraction of GPLs and their weight fraction  $W_{\text{GPL}}$  can be expressed by

$$\frac{W_{\text{GPL}}}{W_{\text{GPL}} + \frac{\rho_{\text{GPL}}}{\rho_{\text{M}}} - \frac{\rho_{\text{GPL}}}{\rho_{\text{M}}} W_{\text{GPL}}} \int_{-h/2}^{h/2} (1 - e_m \lambda(z)) dz \quad (13)$$

$$= \int_{-h/2}^{h/2} V_{\text{GPL}} (1 - e_m \lambda(z)) dz$$

In which  $\rho_{\text{GPL}}$  and  $\rho_{\text{M}}$  are mass density of GPL and metal matrix, respectively. Based on Halpin-Tsai micromechanical model, it is possible to obtain material properties of GPL-reinforced metal matrix structures

$$E_1 = \frac{3}{8} \left( \frac{1 + \xi_{\text{L}}^{\text{GPL}} \eta_{\text{L}}^{\text{GPL}} V_{\text{GPL}}}{1 - \eta_{\text{L}}^{\text{GPL}} V_{\text{GPL}}} \right) E_{\text{M}} + \quad (14)$$

$$\frac{5}{8} \left( \frac{1 + \xi_{\text{W}}^{\text{GPL}} \eta_{\text{W}}^{\text{GPL}} V_{\text{GPL}}}{1 - \eta_{\text{W}}^{\text{GPL}} V_{\text{GPL}}} \right) E_{\text{M}}$$

in which  $E_{\text{m}}$  is Young's modulus of the metal and

$$\xi_{\text{L}}^{\text{GPL}} = 2l_{\text{GPL}}/t_{\text{GPL}}, \eta_{\text{L}}^{\text{GPL}} = \frac{(E_{\text{GPL}}/E_{\text{M}}) - 1}{(E_{\text{GPL}}/E_{\text{M}}) + \xi_{\text{L}}^{\text{GPL}}}, \quad (15)$$

$$\xi_{\text{W}}^{\text{GPL}} = 2w_{\text{GPL}}/t_{\text{GPL}}, \eta_{\text{W}}^{\text{GPL}} = \frac{(E_{\text{GPL}}/E_{\text{M}}) - 1}{(E_{\text{GPL}}/E_{\text{M}}) + \xi_{\text{W}}^{\text{GPL}}}$$

in which  $w_{\text{GPL}}$ ,  $l_{\text{GPL}}$  and  $t_{\text{GPL}}$  denote GPLs' average width, length, and thickness, respectively. Finally, Poisson's ratio of GPL-reinforced metal matrix implementing rule of mixture can be expressed by

$$v_1 = v_{\text{GPL}} V_{\text{GPL}} + v_{\text{M}} V_{\text{M}} \quad (16)$$

where  $V_{\text{M}}$  is the volume fraction of metal matrix ( $V_{\text{M}} = 1 - V_{\text{GPL}}$ ).

#### 4. Theoretical formulations

The mechanical constitutive relations that relate the stresses to the strains are as follows (Fung and Tong 2001)

$$\sigma_{ij} = \lambda \varepsilon_{kk} \delta_{ij} + 2\mu \varepsilon_{ij} \quad (17)$$

where  $\lambda$  and  $\mu$  are the Lamé constants,  $\varepsilon_{ij}$  is the infinitesimal strain tensor and  $\delta_{ij}$  is the Kronecker delta. In the absence of body forces, the equations of motion are as follows

$$\frac{\partial \sigma_x}{\partial x} + \frac{\partial \tau_{xy}}{\partial y} + \frac{\partial \tau_{xz}}{\partial z} = \rho \frac{\partial^2 u}{\partial t^2},$$

$$\frac{\partial \tau_{xy}}{\partial x} + \frac{\partial \sigma_y}{\partial y} + \frac{\partial \tau_{yz}}{\partial z} = \rho \frac{\partial^2 v}{\partial t^2}, \quad (18)$$

$$\frac{\partial \tau_{xz}}{\partial x} + \frac{\partial \tau_{yz}}{\partial y} + \frac{\partial \sigma_z}{\partial z} = \rho \frac{\partial^2 w}{\partial t^2}$$

The infinitesimal strain tensor is related to the displacements as follows

$$\varepsilon_x = \frac{\partial u}{\partial x}, \varepsilon_y = \frac{\partial v}{\partial y}, \varepsilon_z = \frac{\partial w}{\partial z}, \gamma_{xy} = \frac{\partial u}{\partial y} + \frac{\partial v}{\partial x}, \quad (19)$$

$$\gamma_{xz} = \frac{\partial u}{\partial z} + \frac{\partial w}{\partial x}, \gamma_{yz} = \frac{\partial v}{\partial z} + \frac{\partial w}{\partial y}$$

where  $u$ ,  $v$  and  $w$  are displacement components along the  $x$ ,  $y$  and  $z$  axes, respectively. Upon substitution (20) into (18) and then into (19), the equations of motion are obtained in terms of displacement components. The related boundary conditions at  $z = -h/2$  and  $h/2$  are as follow

$$\sigma_{zx} = 0, \sigma_{zy} = 0, \sigma_{zz} = 0 \quad (20)$$

Different types of classical boundary conditions at the edges of the plate can be stated as

-Simply supported (S)

$$\sigma_{yy} = 0, w = 0, u = 0; \quad (21)$$

-Clamped (C)

$$u = 0, v = 0, w = 0; \quad (22)$$

-Free (F)

$$\sigma_{yy} = 0, \sigma_{xy} = 0, \sigma_{yz} = 0 \quad (23)$$

Here, plates with two opposite edges at  $x = -a/2$  and  $a/2$  simply supported and arbitrary conditions at edges  $y = -b/2$  and  $b/2$  are considered. For free vibration analysis, by adopting the following form for the displacement components the boundary conditions at edges  $x = -a/2$  and  $a/2$  are satisfied

$$u(x, y, z, t) = U_m(y, z, t) \cos(m\pi(x + a/2)/a) e^{i\omega t},$$

$$v(x, y, z, t) = V_m(y, z, t) \sin(m\pi(x + a/2)/a) e^{i\omega t}, \quad (24)$$

$$w(x, y, z, t) = W_m(y, z, t) \sin(m\pi(x + a/2)/a) e^{i\omega t}$$

where  $m$  is the wave number along the  $x$ - direction,  $\omega$  is the natural frequency and  $i (= \sqrt{-1})$  is the imaginary number. Substituting for displacement components from (24) into the equations of motion which obtained in terms of displacement components, the coupled partial differential equations are reduced to a set of coupled ordinary differential equations (ODE). The geometrical and natural boundary can also be simplified, however, for brevity purpose they are not shown here.

#### 5. DQM solution for equations of motion and boundary conditions

It is necessary to develop appropriate methods to investigate the mechanical responses of continuously graded carbon nanotube-reinforced structures. But, due to the complexity of the problem, it is difficult to obtain the exact solution. In this paper, the differential quadrature method (DQM) approach is used to solve the governing equations of continuously graded carbon nanotube-

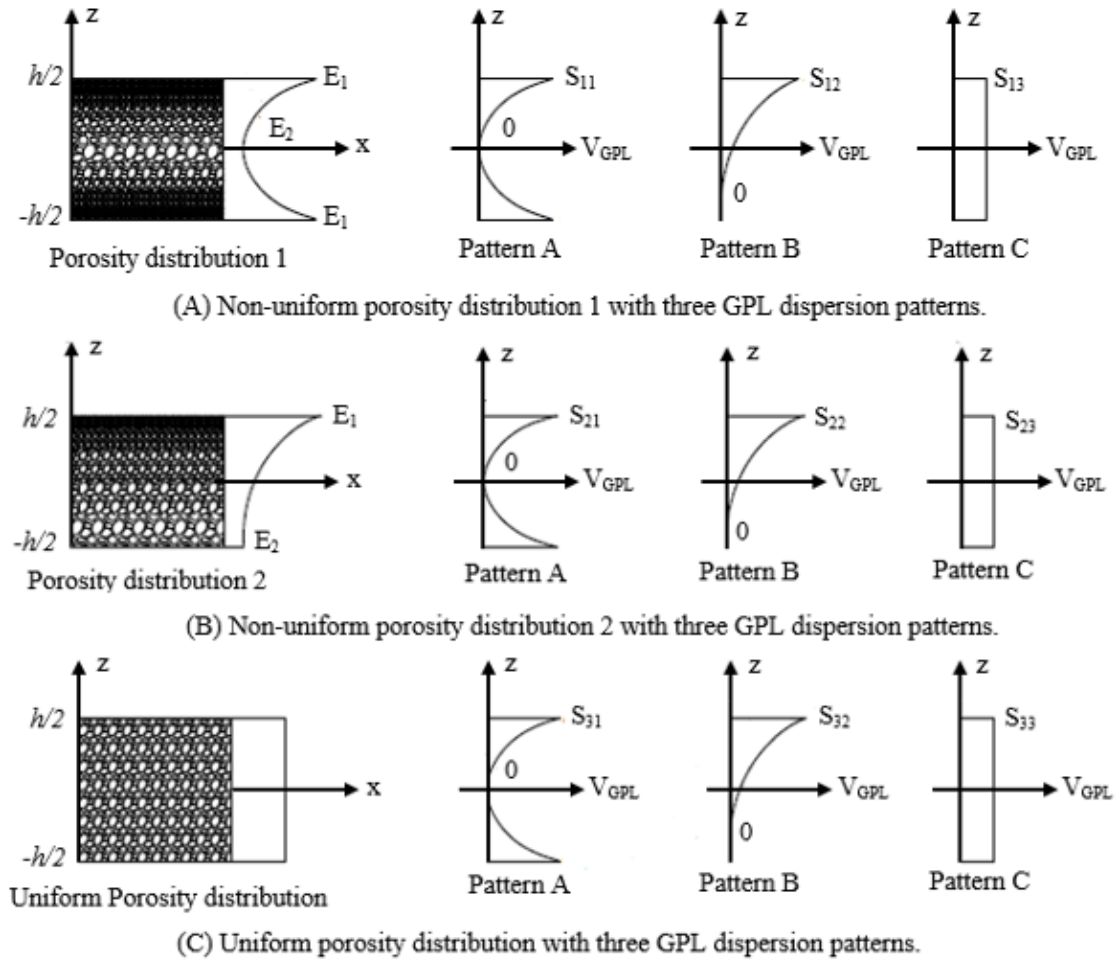


Fig. 2 Porosity distribution and GPL dispersion patterns

reinforced rectangular plates. One can compare DQM solution procedure with the other two widely used traditional methods for plate analysis, i.e., Rayleigh-Ritz method and FEM. The main difference between the DQM and the other methods is how the governing equations are discretized. In DQM the governing equations and boundary conditions are directly discretized, and thus elements of stiffness and mass matrices are evaluated directly. But in Rayleigh-Ritz and FEMs, the weak form of the governing equations should be developed and the boundary conditions are satisfied in the weak form. Generally by doing so larger number of integrals with increasing amount of differentiation should be done to arrive at the element matrices. Also, the number of degrees of freedom will be increased for an acceptable accuracy. The basic idea of the DQM is the derivative of a function, with respect to a space variable at a given sampling point, is approximated as a weighted linear sum of the sampling points in the domain of that variable. In order to illustrate the DQ approximation, consider a function defined on a rectangular domain and the boundary conditions. As a result, at each domain grid point with  $j=2, \dots, N_y-1$  and  $k=2, \dots, N_z-1$ , the discretized equations take the following forms

$$\begin{aligned}
 & -(c_{11})_{jk} \left(\frac{m\pi}{a}\right)^2 U_{mjk} + (c_{12})_{jk} \left(\frac{m\pi}{a}\right) \\
 & \sum_{n=1}^{N_y} A_{jn}^y V_{mnk} + (c_{13})_{jk} \left(\frac{m\pi}{a}\right) \\
 & \sum_{n=1}^{N_z} A_{kn}^z W_{mjn} + \left(\frac{\partial c_{66}}{\partial y}\right)_{jk} \left(\frac{m\pi}{a}\right) V_{mjk} + \sum_{n=1}^{N_y} A_{jn}^y U_{mnk} \\
 & + (c_{66})_{jk} \left(\frac{m\pi}{a}\right) \sum_{n=1}^{N_y} A_{jn}^y V_{mnk} + \sum_{n=1}^{N_z} B_{jn}^y U_{mnk} \\
 & + \left(\frac{\partial c_{55}}{\partial z}\right)_{jk} \left(\frac{m\pi}{a}\right) W_{mjk} + \sum_{n=1}^{N_z} A_{kn}^z U_{mjn} \\
 & + (c_{55})_{jk} \left(\frac{m\pi}{a}\right) \sum_{n=1}^{N_z} A_{kn}^z W_{mjn} + \sum_{n=1}^{N_z} B_{kn}^z U_{mjn} \\
 & = -\rho_{jk} \omega^2 U_{mjk}
 \end{aligned} \tag{25}$$

$$\begin{aligned}
& (c66)_{jk} \left( -\left(\frac{m\pi}{a}\right)^2 V_{mjk} + \left(\frac{-m\pi}{a}\right) \sum_{n=1}^{N_y} A_{jn}^y U_{mnk} \right) \\
& + \left(\frac{\partial c12}{\partial y}\right)_{jk} \left(\frac{-m\pi}{a}\right) U_{mjk} + (c12)_{jk} \left(\left(\frac{-m\pi}{a}\right) \sum_{n=1}^{N_y} A_{jn}^y U_{mnk} \right) \\
& + \left(\frac{\partial c22}{\partial y}\right)_{jk} \left(\sum_{n=1}^{N_y} A_{jn}^y V_{mnk}\right) + (c22)_{jk} \sum_{n=1}^{N_y} B_{jn}^y V_{mnk} \\
& + \left(\frac{\partial c23}{\partial y}\right)_{jk} \left(\sum_{n=1}^{N_z} A_{kn}^z W_{mjn}\right) + (c23)_{jk} \\
& \left(\sum_{n=1}^{N_y} \sum_{r=1}^{N_z} A_{kr}^z A_{jn}^y W_{mnr}\right) + \left(\frac{\partial c44}{\partial z}\right)_{jk} \left(\sum_{n=1}^{N_z} A_{kn}^z V_{mjn}\right) \\
& + \sum_{n=1}^{N_y} A_{jn}^y W_{mnk} + (c44)_{jk} \left(\sum_{n=1}^{N_z} B_{kn}^z V_{mjn}\right) \\
& + \sum_{n=1}^{N_y} \sum_{r=1}^{N_z} A_{kr}^z A_{jn}^y W_{mnr} \\
& = -\rho_{jk} \omega^2 V_{mjk} \\
& (c55)_{jk} \left( -\left(\frac{m\pi}{a}\right)^2 W_{mjk} - \frac{m\pi}{a} \sum_{n=1}^{N_z} A_{kn}^z U_{mjn} \right) \\
& + \left(\frac{\partial c44}{\partial y}\right)_{jk} \left(\sum_{n=1}^{N_z} A_{kn}^z V_{mjn} + \sum_{n=1}^{N_y} A_{jn}^y W_{mnk}\right) \\
& + (c44)_{jk} \left(\sum_{n=1}^{N_y} \sum_{r=1}^{N_z} A_{kr}^z A_{jn}^y V_{mnr} + \sum_{n=1}^{N_y} B_{jn}^y W_{mnk}\right) \\
& + \left(\frac{\partial c13}{\partial z}\right)_{jk} \left(-\frac{m\pi}{a} U_{mjk}\right) + (c13)_{jk} \\
& \left(-\frac{m\pi}{a} \sum_{n=1}^{N_z} A_{kn}^z U_{mjn}\right) + \left(\frac{\partial c23}{\partial z}\right)_{jk} \\
& \sum_{n=1}^{N_y} A_{jn}^y V_{mnk} + (c23)_{jk} \sum_{n=1}^{N_y} \sum_{r=1}^{N_z} A_{kr}^z A_{jn}^y V_{mnr} + \left(\frac{\partial c33}{\partial z}\right)_{jk} \\
& \sum_{n=1}^{N_z} A_{kn}^z W_{mjn} + (c33)_{jk} \sum_{n=1}^{N_z} B_{kn}^z W_{mjn} \\
& = -\rho_{jk} \omega^2 W_{mjk}
\end{aligned} \tag{26}$$

where  $A_{ij}^y$ ,  $A_{ij}^z$  and  $B_{ij}^y$ ,  $B_{ij}^z$  are the first and second order DQ weighting coefficients in the  $y$ - and  $z$ -directions, respectively. In a similar manner the boundary conditions can be discretized.

In order to carry out the eigenvalue analysis, the domain and boundary nodal displacements should be separated. In vector forms, they are denoted as  $\{d\}$  and  $\{b\}$ , respectively. Based on this definition, the discretized form of the equations of motion and the related boundary conditions can be represented in the matrix form as

$$[[K_{db}][K_{dd}]] \begin{Bmatrix} \{b\} \\ \{d\} \end{Bmatrix} - \omega^2 [M] \{d\} = \{0\} \tag{28}$$

and boundary conditions

$$[K_{bd}] \{d\} + [K_{bb}] \{b\} = \{0\} \tag{29}$$

Eliminating the boundary degrees of freedom in (28) using (29), this equation becomes

$$[K] - \omega^2 [M] \{d\} = \{0\} \tag{30}$$

where  $[K] = [K_{dd}] - [K_{db}][K_{bb}]^{-1}[K_{bd}]$ . The above eigenvalue system of equations can be solved to find the natural frequencies and mode shapes of the plate.

## 6. Convergence and comparison studies

Firstly, the results are compared with those of 1-D conventional functionally graded rectangular plates, and then, the results of the presented formulations are given in the form of convergence studies with respect to  $N_z$  and  $N_y$ , the number of discrete points distributed along the thickness and width of the plate, respectively. The boundary conditions of the plate are specified by the letter symbols, for example, S-C-S-F denotes a plate with edges  $x=-a/2$  and  $a/2$  simply supported (S), edge  $y=-b/2$  clamped (C) and edge  $y=b/2$  free (F). As an example to study the accuracy of the presented method, In Table 1, the first seven non-dimensional natural frequency parameters of simply supported thick FG plate are compared with those of Matsunaga (2008) and Yas and Sobhani (2010). According to the data presented in the table 1, excellent solution agreements can be observed between the present method and those of the other methods. Based on the above studies, a numerical value of  $N_z = N_y = 13$  is used for the next studies. The material property and geometry parameters of GPLs are  $W_{GPL}=1.5 \mu\text{m}$ ,  $l_{GPL}=2.5 \mu\text{m}$ ,  $t_{GPL} 1.5 \text{ nm}$ ,  $E_{GPL}=1.01 \text{ TPa}$ ,  $\rho_{GPL}=1062.5 \text{ kg/m}^3$ ,  $\nu=0.186$  (Rafiee et al. 2009, Liu et al. 2007), and the material properties of metal are  $E_M = 130 \text{ GPa}$ ,  $\rho_M = 8960 \text{ kg/m}^3$ ,  $\nu_M = 0.34$  (Kitipornchai et al. 2017).

In this study, the non-dimensional natural frequency is as follows

$$\Omega = \omega \frac{b^2}{\pi^2} \sqrt{\rho_m h / D_m}, D_m = E_m h^3 / 12(1 - \nu_m^2) \tag{31}$$

where  $\rho_M$ ,  $E_M$  and  $\nu_M$  are mechanical properties of Copper.

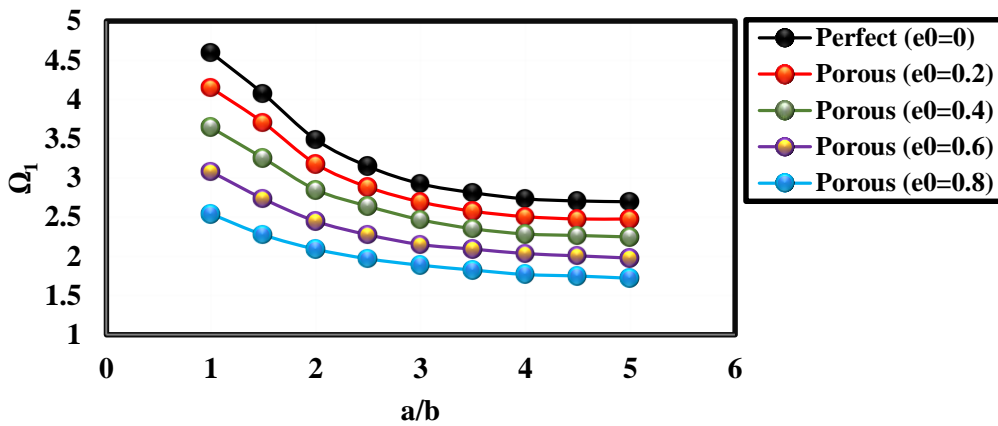


Fig. 3 Variation of natural frequency of Uniform GPL-reinforced plates versus length-to-width ratio ( $a/b$ ) for SCSC boundary condition (1 wt. %)

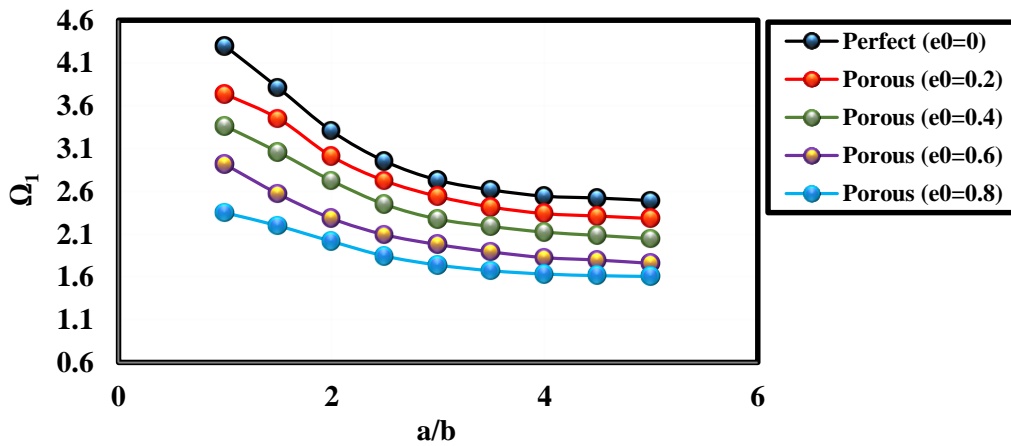


Fig. 4 Variation of natural frequency of Uniform GPL-reinforced plates versus length-to-width ratio ( $a/b$ ) for SSSS boundary condition (1 wt. %)

### 7. Benchmark results

Influences of porosity coefficient on vibration frequency of GPL reinforced rectangular plate with respect to length-to-width ratio ( $a/b$ ) is shown in Figs. 3, 4 and 5. It is clear that a porous nanocomposite plate has lower natural frequencies than a perfect plate ( $e_0=0$ ). In other words, increasing porosity coefficient results in smaller natural frequencies due to the reduction in the bending rigidity of the nanocomposite plate. Therefore, for better understanding of mechanical behavior of nanocomposite plates, it is crucial to consider porosities inside the material structure. One can also see that vibration frequencies are significantly decreased with the increasing in length-to-width ratio ( $a/b$ ). This is because nanocomposite plates with higher length-to-width ratio ( $a/b$ ) are more flexible leading to smaller vibration frequencies.

The combined effects of porosity distribution and GPL distribution pattern on the fundamental frequency are investigated in Fig. 6 in which the fundamental natural frequency at various GPL weight fractions is presented. Symmetric GPL pattern A is proved to be the best dispersion method, followed by the uniform pattern C which is slightly better than the asymmetric pattern B. Results indicate that plate with non-uniform symmetric porosity distribution 1 and symmetric GPL pattern A have the largest fundamental frequencies, i.e., the highest effective stiffness under the same GPL weight fraction, suggesting that a nanocomposite plate in which both internal pores and nanofillers are symmetrically distributed can offer the best structural performance. It should be noted this tendency has been seen in other types of boundary conditions but for the sake of brevity, they are not reported here.

Table 1 Convergence behavior and accuracy of the first seven non-dimensional natural frequencies ( $\varpi = \omega h \sqrt{\rho_c / E_c}$ ) of a simply supported FG plate against the number of DQ grid points ( $b/h = 2$ ).

$P$	$N_z$	$N_y$	$\varpi_1$	$\varpi_2$	$\varpi_3$	$\varpi_4$	$\varpi_5$	$\varpi_6$	$\varpi_7$	
0	7	7	0.5569	0.9395	0.9735	1.3764	1.5072	1.6064	1.7384	
		9	0.5570	0.9396	0.9741	1.3771	1.5083	1.6071	1.7401	
		13	0.5570	0.9396	0.9740	1.3774	1.5088	1.6076	1.7407	
	9	7	0.5573	0.9398	0.9735	1.3771	1.5087	1.6074	1.7403	
		9	0.5572	0.9400	0.9742	1.3777	1.5090	1.6079	1.7406	
		13	0.5572	0.9400	0.9741	1.3778	1.5096	1.6086	1.7405	
	13	7	0.5571	0.9401	0.9735	1.3779	1.5094	1.6083	1.7411	
		9	0.5572	0.9400	0.9742	1.3777	1.5090	1.6078	1.7405	
		13	0.5572	0.9400	0.9742	1.3777	1.5090	1.6078	1.7406	
	0.5	7	Matsunaga (2008)	0.5572	0.9400	0.9742	1.3777	1.5090	1.6078	1.7406
			Yas and SobhaniAragh (2010)	0.557243	0.940041	-	-	1.508987	-	1.740602
			7	0.4829	0.8222	0.8700	1.2250	1.3332	1.4364	1.5401
9		9	0.4828	0.8229	0.8707	1.2258	1.3337	1.4367	1.5429	
		13	0.4830	0.8224	0.8706	1.2254	1.3338	1.4370	1.5424	
		7	0.4833	0.8225	0.8701	1.2251	1.3335	1.4365	1.5402	
13		9	0.4835	0.8240	0.8708	1.2257	1.3340	1.4370	1.5431	
		13	0.4836	0.8233	0.8707	1.2258	1.3340	1.4369	1.5426	
		7	0.4836	0.8227	0.8701	1.2251	1.3334	1.4366	1.5402	
1		7	9	0.4835	0.8231	0.8708	1.2259	1.3338	1.4370	1.5431
			13	0.4835	0.8233	0.8709	1.2259	1.3339	1.4370	1.5425
			Matsunaga (2008)	0.4835	0.8233	0.8709	1.2259	1.3339	1.4370	1.5425
	9	Yas and SobhaniAragh (2010)	0.482849	0.822358	-	-	1.332605	-	1.541085	
		7	0.4367	0.7476	0.7997	1.1158	1.2154	1.3085	1.4059	
		9	0.4374	0.7477	0.8001	1.1165	1.2159	1.3090	1.4075	
	13	13	0.4373	0.7478	0.8005	1.1163	1.2162	1.3088	1.4077	
		7	0.4368	0.7477	0.7998	1.1159	1.2157	1.3088	1.4068	
		9	0.4374	0.7477	0.8003	1.1165	1.2161	1.3090	1.4076	
	4	7	13	0.4374	0.7478	0.8006	1.1165	1.2162	1.3090	1.4078
			7	0.4368	0.7477	0.7999	1.1159	1.2158	1.3088	1.4070
			9	0.4375	0.7478	0.8003	1.1165	1.2162	1.3091	1.4076
9		13	0.4375	0.7478	0.8005	1.1165	1.2163	1.3091	1.4077	
		7	0.4375	0.7477	0.8005	1.1166	1.2163	1.3091	1.4078	
		9	0.437396	0.747514	-	-	1.216035	-	1.407459	
10		7	7	0.3565	0.5988	0.6249	0.8724	0.9589	1.0000	1.1029
			9	0.3577	0.5995	0.6355	0.8729	0.9589	1.0007	1.1038
			13	0.3577	0.5996	0.6349	0.8728	0.9589	1.0003	1.1030
		9	7	0.3569	0.5989	0.6250	0.8726	0.9589	1.0001	1.1032
			9	0.3579	0.5997	0.6357	0.8731	0.9589	1.0008	1.1040
			13	0.3578	0.5997	0.6351	0.8730	0.9589	1.0005	1.1032
	13	7	0.3571	0.5991	0.6252	0.8727	0.9589	1.0001	1.1033	
		9	0.3579	0.5997	0.6357	0.8731	0.9589	1.0008	1.1040	
		13	0.3579	0.5997	0.6352	0.8731	0.9589	1.0008	1.1040	
	10	7	Matsunaga (2008)	0.3579	0.5997	0.6352	0.8731	0.9591	1.0008	1.1040
			Yas and SobhaniAragh (2010)	0.357758	0.599494	-	-	0.958764	-	1.103674
			7	0.3306	0.5454	0.5657	0.7866	0.8588	0.9043	0.9838
9		9	0.3311	0.5460	0.5662	0.7890	0.8588	0.9047	0.9841	
		13	0.3310	0.5459	0.5661	0.7881	0.8588	0.9050	0.9846	
		7	0.3308	0.5455	0.5659	0.7870	0.8588	0.9044	0.9840	
13		9	0.3313	0.5461	0.5664	0.7892	0.8588	0.9048	0.9842	
		13	0.3312	0.5460	0.5663	0.7883	0.8588	0.9051	0.9846	
		7	0.3309	0.5455	0.5660	0.7871	0.8588	0.9045	0.9840	
10		7	9	0.3313	0.5461	0.5664	0.7892	0.8588	0.9049	0.9844
			13	0.3313	0.5461	0.5664	0.7884	0.8588	0.9051	0.9847
			Matsunaga (2008)	0.3313	0.5460	0.5664	0.7885	0.8588	0.9050	0.9847
	9	Yas and SobhaniAragh (2010)	0.331146	0.545833	-	-	0.858445	-	0.984365	
		7	0.3306	0.5454	0.5657	0.7866	0.8588	0.9043	0.9838	
		9	0.3311	0.5460	0.5662	0.7890	0.8588	0.9047	0.9841	
	13	13	0.3310	0.5459	0.5661	0.7881	0.8588	0.9050	0.9846	
		7	0.3308	0.5455	0.5659	0.7870	0.8588	0.9044	0.9840	
		9	0.3313	0.5461	0.5664	0.7892	0.8588	0.9048	0.9842	
	10	7	13	0.3312	0.5460	0.5663	0.7883	0.8588	0.9051	0.9846
			7	0.3309	0.5455	0.5660	0.7871	0.8588	0.9045	0.9840
			9	0.3313	0.5461	0.5664	0.7892	0.8588	0.9049	0.9844
9		13	0.3313	0.5461	0.5664	0.7884	0.8588	0.9051	0.9847	
		Matsunaga (2008)	0.3313	0.5460	0.5664	0.7885	0.8588	0.9050	0.9847	
		Yas and SobhaniAragh (2010)	0.331146	0.545833	-	-	0.858445	-	0.984365	

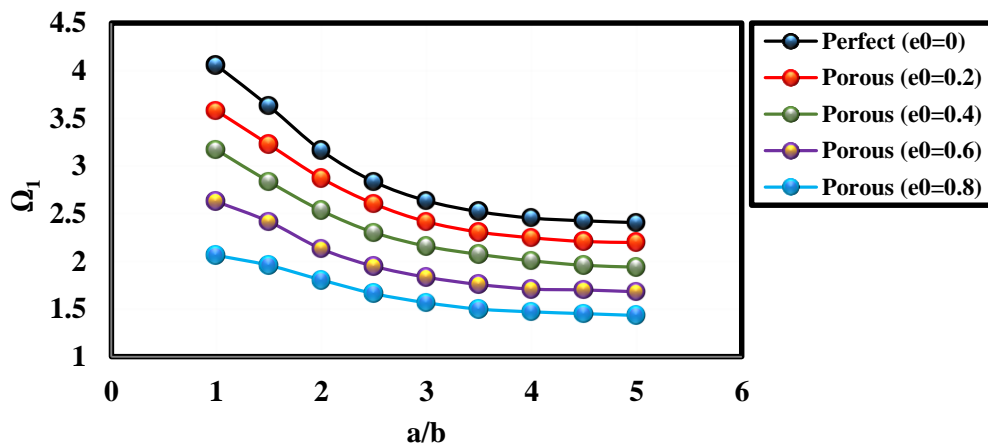


Fig. 5 Variation of natural frequency of Uniform GPL-reinforced plates versus length-to-width ratio ( $a/b$ ) for SFSF boundary condition (1 wt. %)

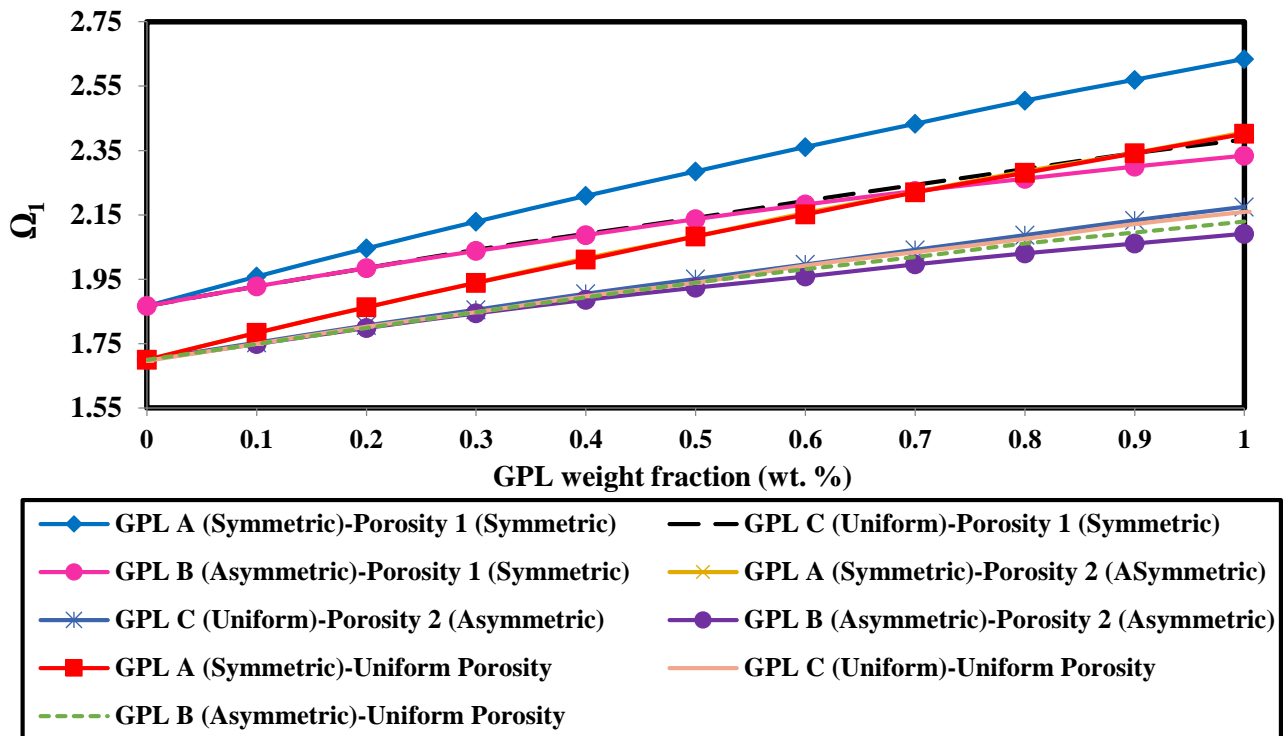


Fig. 6 Effect of GPL on the fundamental frequency of nanocomposite SCSC rectangular plate ( $e_0=0.5$ ,  $a/b=4$ ).

### 8. Conclusions

This paper deals with vibration analysis of functionally graded porous nanocomposite plate where the internal pores and graphene platelets (GPLs) are distributed in the matrix uniformly or non-uniformly according to three different patterns. The 2-D differential quadrature method as an efficient and accurate numerical tool is used to discretize the governing equations and to implement the boundary conditions. The influence of boundary conditions, length-to-width ratio ( $a/b$ ) and dispersion pattern of GPLs on the fundamental

frequency of the FG plates are investigated. From this study some conclusions can be made as following:

- It is observed that a porous nanocomposite plate has lower natural frequencies than a perfect plate ( $e_0=0$ ).
- Vibration frequencies are significantly decreased with the increasing in length-to-width ratio ( $a/b$ ).
- According to the results, Symmetric GPL pattern A is proved to be the best dispersion method,

followed by the uniform pattern C which is slightly better than the asymmetric pattern B.

- It is observed that plate with non-uniform symmetric porosity distribution 1 and symmetric GPL pattern A have the largest fundamental frequencies.

Results show that for better understanding of mechanical behavior of nanocomposite plates, it is crucial to consider porosities inside the material structure

## Acknowledgments

The research described in this paper was financially supported by the National Natural Science Foundation of China (No. 51378377) and National Natural Science Foundation of China (No. 41872001).

## References

- Ahmed Houari, M.S., Bessaim, A., Bernard, F., Tounsi, A. and Mahmoud, S.R. (2018), "Buckling analysis of new quasi-3D FG nanobeams based on nonlocal strain gradient elasticity theory and variable length scale parameter", *Steel Compos. Struct.*, **28**(1), 13-24. <https://doi.org/10.12989/scs.2018.28.1.013>.
- Alibeigloo, A. (2013), "Three-dimensional free vibration analysis of multi-layered graphene sheets embedded in elastic matrix", *J.V.C.*, **19**(16), 2357-2371. <https://doi.org/10.1177/1077546312456056>.
- Arefi, M. (2015), "Elastic solution of a curved beam made of functionally graded materials with different cross sections", *Steel Compos. Struct.*, **18**(3), 659-672. <http://dx.doi.org/10.12989/scs.2015.18.3.659>.
- Barka, M., Benrahou, K.H., Bakora, A. and Tounsi, A. (2016), "Thermal post-buckling behavior of imperfect temperature-dependent sandwich FGM plates resting on Pasternak elastic foundation", *Steel Compos. Struct.*, **22**(1), 91-112. <https://doi.org/10.12989/scs.2016.22.1.091>.
- Bennai, R., AitAtmane, H. and Tounsi, A. (2015), "A new higher-order shear and normal deformation theory for functionally graded sandwich beams", *Steel Compos. Struct.*, **19**(3), 521-546. <https://doi.org/10.12989/scs.2015.19.3.521>.
- Benveniste, Y. (1987), "A new approach to the application of Mori-Tanaka's theory in composite materials", *Mech. Mater.*, **6**(2), 147-157. [https://doi.org/10.1016/0167-6636\(87\)90005-6](https://doi.org/10.1016/0167-6636(87)90005-6).
- Bert, C.W. and Malik, M. (1996), "Differential quadrature method in computational mechanics: a review", *Appl. Mech. Review.*, **49**(1), 1-28.
- Bonnet, P., Sireude, D., Garnier, B. and Chauvet, O. (2007), "Thermal properties and percolation in carbon nanotube-polymer composites", *J. Appl. Phys.*, **91**(20), 2019-2030. <https://doi.org/10.1063/1.2813625>.
- Bouchafa, A., Bouiadjra, M.B., Houari, M.S.A. and Tounsi, A. (2015), "Thermal stresses and deflections of functionally graded sandwich plates using a new refined hyperbolic shear deformation theory", *Steel Compos. Struct.*, **18**(6), 1493-1515. <https://doi.org/10.12989/scs.2015.18.6.1493>.
- Bouguenina, O., Belakhdar, K., Tounsi, A. and Bedia, E.A.A. (2015), "Numerical analysis of FGM plates with variable thickness subjected to thermal buckling", *Steel Compos. Struct.*, **19**(3), 679-695. <http://dx.doi.org/10.12989/scs.2015.19.3.679>.
- Chang, T. and Gao, H. (2003), "Size-dependent elastic properties of a single-walled carbon nanotube via a molecular mechanics model", *J. Mech. Phys. Solids*, **51**(6), 1059-1074. [https://doi.org/10.1016/S0022-5096\(03\)00006-1](https://doi.org/10.1016/S0022-5096(03)00006-1).
- Chen, C.H. and Cheng, C.H. (1996), "Effective elastic moduli of misoriented short-fiber composites", *Int. J. Solids Struct.*, **33**(17), 2519-2539. [https://doi.org/10.1016/0020-7683\(95\)00160-3](https://doi.org/10.1016/0020-7683(95)00160-3).
- Chen, C.S., Liu, F.H. and Chen, W.R. (2017), "vibration and stability of initially stressed sandwich plates with FGM face sheets in thermal environments", *Steel Compos. Struct.*, **23**(3), 251-261. <https://doi.org/10.12989/scs.2017.23.3.251>.
- Chen, D., Yang, J. and Kitipornchai, S. (2015), "Elastic buckling and static bending of shear deformable functionally graded porous beam", *Compos. Struct.*, **133**, 54-61. <https://doi.org/10.1016/j.compstruct.2015.07.052>.
- Cheng, Z.Q. and Batra, R. (2000), "Exact correspondence between eigenvalues of membranes and functionally graded simply supported polygonal plates", *J. Sound Vib.*, **229**(4), 879-895. <https://doi.org/10.1006/jsvi.1999.2525>.
- Endo, M., Hayashi, T., Kim, Y.A., Terrones, M. and Dresselhaus, M.S. (2004), "Applications of carbon nanotubes in the twenty-first century", *Philos. T. R. Soc. Lond., Series A: Mathematical, Physical and Engineering Sciences*, **362**, 2223-2238. <https://doi.org/10.1098/rsta.2004.1437>.
- Esawi, A.M. and Farag, M.M. (2007), "Carbon nanotube reinforced composites: potential and current challenges", *Mater. Des.*, **28**(9), 2394-2401. <https://doi.org/10.1016/j.matdes.2006.09.022>.
- Eshelby, J.D. (1957), "The determination of the elastic field of an ellipsoidal inclusion, and related problems", *Proc. R. Soc. London, Ser. A.*, **241**(1226), 376-396. <https://doi.org/10.1098/rspa.1957.0133>.
- Eshelby, J.D. (1959), "The elastic field outside an ellipsoidal inclusion", *Proc. R. Soc. London, Ser. A.*, **252**(1271), 561-569. <https://doi.org/10.1098/rspa.1959.0173>.
- Fidelus, J., Wiesel, E., Gojny, F., Schulte, K. and Wagner, H. (2005), "Thermo-mechanical properties of randomly oriented carbon/epoxy nanocomposites", *Compos. Part A: Appl. Sci. Manuf.*, **36**(11), 1555-1561. <https://doi.org/10.1016/j.compositesa.2005.02.006>.
- Formica, G., Lacarbonara, W. and Alessi, R. (2010), "Vibrations of carbon nanotube-reinforced composites", *J. Sound Vib.*, **329**(10), 1875-1889. <https://doi.org/10.1016/j.jsv.2009.11.020>.
- Fung, Y.C. and Tong, P. (2001), "Classical and computational solid mechanics", 5, World scientific Singapore.
- Giordano, S., Palla, P. and Colombo, L. (2009), "Nonlinear elasticity of composite materials", *Eur. Phys. J. B. Condensed Matter and Complex systems*, **68**(89), 89-101. <https://doi.org/10.1140/epjb/e2009-00063-1>.
- Han, Y. and Elliott, J. (2007), "Molecular dynamics simulations of the elastic properties of polymer/carbon nanotube composites", *Comput. Mater. Sci.*, **39**(2), 315-323. <https://doi.org/10.1016/j.commatsci.2006.06.011>.
- Hassan, M., Marin, M., Ellahi, R. and Alamri, S.Z. (2018), "Exploration of convective heat transfer and flow characteristics synthesis by Cu-Ag/water hybrid-nanofluids", *Heat Transfer Res.*, **49**(18), 1837-1848. DOI: 10.1615/HeatTransRes.2018025569.
- Hosseini, S. M. and Zhang, C. (2018), "Elastodynamic and wave propagation analysis in a FG Graphene platelets-reinforced nanocomposite cylinder using a modified nonlinear micromechanical model", *Steel Compos. Struct.*, **27**(3), 255-271. <http://dx.doi.org/10.12989/scs.2018.27.3.255>.
- Hu, N., Fukunaga, H., Lu, C., Kameyama, M. and Yan, B. (2005), "Prediction of elastic properties of carbon nanotube reinforced

- composites”, *Proc. R. Soc. London, Ser. A*, **461**(2058), 1685-1710. <https://doi.org/10.1098/rspa.2004.1422>.
- Jabbari, M., Hashemitaheeri, M., Mojahedin, A., Eslami, M.R. (2014), “Thermal buckling analysis of functionally graded thin circular plate made of saturated porous materials”, *J. Therm. Stresses*, **37**(2), 202-220. <https://doi.org/10.1080/01495739.2013.839768>.
- Jabbari, M., Mojahedin, A., Khorshidvand, A.R. and Eslami, M.R. (2013), “Buckling analysis of a functionally graded thin circular plate made of saturated porous materials”, *J. Eng. Mech.*, **140**, 287-295. [https://doi.org/10.1061/\(ASCE\)EM.1943-7889.0000663](https://doi.org/10.1061/(ASCE)EM.1943-7889.0000663).
- Jin, Y. and Yuan, F. (2003), “Simulation of elastic properties of single-walled carbon nanotubes”, *Compos. Sci. Technol.*, **63**(11), 1507-1515. [https://doi.org/10.1016/S0266-3538\(03\)00074-5](https://doi.org/10.1016/S0266-3538(03)00074-5).
- Kitipornchai, S., Chen, D., Yang, J. (2017), “Free vibration and elastic buckling of functionally graded porous beams reinforced by graphene platelets”, *Mater. Design*, **116**, 656-665.
- Liew, K.M., Han, J.B., Xiao, Z. and Du, H. (1996), “Differential quadrature method for Mindlin plates on Winkler foundations”, *Int. J. Mech. Sci.*, **38**(4), 405-421. [https://doi.org/10.1016/0020-7403\(95\)00062-3](https://doi.org/10.1016/0020-7403(95)00062-3).
- Liu, F., Ming, P. and Li, J. (2007), “Ab initio calculation of ideal strength and phonon instability of graphene under tension”, *Physical Review B*, **76**, 064120. <https://doi.org/10.1103/PhysRevB.76.064120>.
- Liu, R. and Wang, L. (2015), “Thermal vibration of a single-walled carbon nanotube predicted by semiquantum molecular dynamics”, *Physical Chemistry Chemical Physics*, **7**.
- Marin, M., Agarwal, R.P. and Mahmoud, S.R. (2013), “Nonsimple material problems addressed by the Lagrange’s identity”, *Bound. Value Probl.*, **135**, 1-14. <https://doi.org/10.1186/1687-2770-2013-135>.
- Marin, M., Baleanu, D. and Vlasie, S. (2017), “Effect of microtemperatures for micropolar thermoelastic bodies”, *Struct. Eng. Mech.*, **61**(3), 381-387. <https://doi.org/10.12989/sem.2017.61.3.381>.
- Marin, M. and Craciun, E.M. (2017), “Uniqueness results for a boundary value problem in dipolar thermoelasticity to model composite materials”, *Compos. Part B: Eng.*, **126**, 27-37. <https://doi.org/10.1016/j.compositesb.2017.05.063>.
- Matsunaga, H. (2000), “Vibration and stability of thick plates on elastic foundations”, *J. Eng. Mech.-ASCE*, **126**(1), 27-34. [https://doi.org/10.1061/\(ASCE\)0733-9399\(2000\)126:1\(27\)](https://doi.org/10.1061/(ASCE)0733-9399(2000)126:1(27)).
- Matsunaga, H. (2008), “Free vibration and stability of functionally graded plates according to a 2-D higher-order deformation theory”, *Compos. Struct.*, **82**(4), 499-512. <https://doi.org/10.1016/j.compstruct.2007.01.030>.
- Moniruzzaman, M. and Winey, K.I. (2006), “Polymer nanocomposites containing carbon nanotubes”, *Macromolecules*, **39**(16), 5194-5205. <https://doi.org/10.1021/ma060733p>.
- Moradi-Dastjerdi, R. and Momeni-Khabisi, H. (2016), “Dynamic analysis of functionally graded nanocomposite plates reinforced by wavy carbon nanotube”, *Steel Compos. Struct.*, **22**(2), 277-299. <http://dx.doi.org/10.12989/scs.2016.22.2.277>.
- Mori, T. and Tanaka, K. (1973), “Average stress in matrix and average elastic energy of materials with misfitting inclusions”, *Acta Metall.*, **21**(5), 571-574. [https://doi.org/10.1016/0001-6160\(73\)90064-3](https://doi.org/10.1016/0001-6160(73)90064-3).
- Mura, T. (1987), *Micromechanics of defects in solids*, 3, Springer Science & Business Media.
- Odegard, G., Gates, T., Wise, K., Park, C. and Siochi, E. (2003), “Constitutive modeling of nanotube-reinforced polymer composites”, *Compos. Sci. Technol.*, **63**(11), 1671-1687. [https://doi.org/10.1016/S0266-3538\(03\)00063-0](https://doi.org/10.1016/S0266-3538(03)00063-0).
- Othman, M.I.A. and Marin, M. (2017), “Effect of thermal loading due to laser pulse on thermoelastic porous medium under G-N theory”, *Results in Physics*, **7**, 3863-3872. <https://doi.org/10.1016/j.rinp.2017.10.012>.
- Park, W.T., Han, S.C., Jung, W.Y. and Lee, W.H. (2016), “Dynamic instability analysis for S-FGM plates embedded in Pasternak elastic medium using the modified couple stress theory”, *Steel Compos. Struct.*, **22**(6), 1239-1259. <https://doi.org/10.12989/scs.2016.22.6.1239>.
- Qian, D., Dickey, E.C., Andrews, R. and Rantell, T. (2000), “Load transfer and deformation mechanisms in carbon nanotube-polystyrene composites”, *Appl. Phys. Lett.*, **76**, 2868-2870. <https://doi.org/10.1063/1.126500@apl.2019.APLCLASS2019.is.sue-1>.
- Rafiee, M.A., Rafiee, J., Wang, Z., Song, H., Yu, Z.Z. and Koratkar, N. (2009), “Enhanced mechanical properties of nanocomposites at low graphene content”, *ACS nano*, **3**, 3884-3890. <https://doi.org/10.1021/nn9010472>.
- Salvetat-Delmotte, J.P. and Rubio, A. (2002), “Mechanical properties of carbon nanotubes: a fiber digest for beginners”, *Carbon*, **40**(10), 1729-1734. [https://doi.org/10.1016/S0008-6223\(02\)00012-X](https://doi.org/10.1016/S0008-6223(02)00012-X).
- Shen, H.S. (2009), “Nonlinear bending of functionally graded carbon nanotube-reinforced composite plates in thermal environments”, *Compos. Struct.*, **91**(1), 9-19. <https://doi.org/10.1016/j.compstruct.2009.04.026>.
- Shen, H.S. (2012), “Thermal buckling and postbuckling behavior of functionally graded carbon nanotube-reinforced composite cylindrical shells”, *Compos. Part B: Eng.*, **43**(3), 1030-1038. <https://doi.org/10.1016/j.compositesb.2011.10.004>.
- Shen, H.S. and Zhang, C.L. (2010), “Thermal buckling and postbuckling behavior of functionally graded carbon nanotube-reinforced composite plates”, *Mater. Des.*, **31**(7), 3403-3411. <https://doi.org/10.1016/j.matdes.2010.01.048>.
- Shen, H.S. and Zhu, Z.H. (2010), “Buckling and postbuckling behavior of functionally graded nanotube-reinforced composite plates in thermal environments”, *Comput. Mater. Continua (CMC)*, **18**(2), 155-182.
- Shu, C. and Wang, C. (1999), “Treatment of mixed and nonuniform boundary conditions in GDQ vibration analysis of rectangular plates”, *Eng. Struct.*, **21**(2), 125-134. [https://doi.org/10.1016/S0141-0296\(97\)00155-7](https://doi.org/10.1016/S0141-0296(97)00155-7).
- Tahounh, V. (2016), “Using an equivalent continuum model for 3D dynamic analysis of nanocomposite plates”, *Steel Compos. Struct.*, **20**(3), 623-649. <https://doi.org/10.12989/scs.2016.20.3.623>.
- Tahounh, V., Yas, M.H., Tourang, H. and Kabirian, M. (2013) “Semi-analytical solution for three-dimensional vibration of thick continuous grading fiber reinforced (CGFR) annular plates on Pasternak elastic foundations with arbitrary boundary conditions on their circular edges”, *Meccanica*, **48**(6), 1313-1336. <https://doi.org/10.1007/s11012-012-9669-4>.
- Thostenson, E.T., Ren, Z. and Chou, T.W. (2001), “Advances in the science and technology of carbon nanotubes and their composites: a review”, *Compos. Sci. Technol.*, **61**(13), 1899-1912. [https://doi.org/10.1016/S0266-3538\(01\)00094-X](https://doi.org/10.1016/S0266-3538(01)00094-X).
- Tornabene, F., Baccocchi, M., Fantuzzi, N. and Reddy, J.N. (2018), “Multiscale Approach for Three-Phase CNT/Polymer/Fiber Laminated Nanocomposite Structures”, *Polymer Composites*, In Press, DOI: 10.1002/pc.24520.
- Tornabene, F., Fantuzzi, N., Ubertini, F. and Viola, E. (2015), “Strong formulation finite element method based on differential quadrature: A survey”, *Appl. Mech. Rev.*, **67**(2), 1-55. <https://doi.org/10.1115/1.4028859>.
- Tornabene, F., Fantuzzi, N. and Baccocchi, M. (2019), “Refined shear deformation theories for laminated composite arches and beams with variable thickness: Natural frequency analysis”,

- Eng. Anal. Bound. Elem.*, **100**, 24-47.  
<https://doi.org/10.1016/j.enganabound.2017.07.029>.
- Tornabene, F., Fantuzzi, N. and Baccocchi, M. (2017), "Foam core composite sandwich plates and shells with variable stiffness: Effect of the curvilinear fiber path on the modal response", *J. Sandw. Struct. Mater.*, **21**(1), 320-365.  
<https://doi.org/10.1177/1099636217693623>.
- Valter, B., Ram, M.K. and Nicolini, C. (2002), "Synthesis of multiwalled carbon nanotubes and poly (o-anisidine) nanocomposite material: Fabrication and characterization of its Langmuir-Schaefer films", *Langmuir*, **18**(5), 1535-1541.  
<https://doi.org/10.1021/la0104673>.
- Wang, Z.X. and Shen, H.S. (2011), "Nonlinear vibration of nanotube-reinforced composite plates in thermal environments", *Comput. Mater. Sci.*, **50**(8), 2319-2330.  
<https://doi.org/10.1016/j.commatsci.2011.03.005>.
- Wernik, J. and Meguid, S. (2011), "Multiscale modeling of the nonlinear response of nano-reinforced polymers", *Acta Mech.*, **217**(1), 1-16.
- Wu, C.P. and Liu, Y.C. (2016), "A state space meshless method for the 3D analysis of FGM axisymmetric circular plates", *Steel Compos. Struct.*, **22**(1), 161-182.  
<https://doi.org/10.12989/scs.2016.22.1.161>.
- Xu, W., Wang, L. and Jiang, J. (2016), "Strain gradient finite element analysis on the vibration of double-layered graphene sheets", *Int. J. Comput. Methods*, **13**(3).  
<https://doi.org/10.1142/S0219876216500110>.
- Yas, M.H. and Aragh, B.S. (2010), "Free vibration analysis of continuous grading fiber reinforced plates on elastic foundation", *Int. J. Eng. Sci.*, **48**(12), 1881-1895.  
<https://doi.org/10.1016/j.ijengsci.2010.06.015>.
- Yokozeki, T., Iwahori, Y. and Ishiwata, S. (2007), "Matrix cracking behaviors in carbon fiber/epoxy laminates filled with cup-stacked carbon nanotubes (CSCNTs)", *Compos. Part A: Appl. Sci. Manufact.*, **38**(3), 917-924.  
<https://doi.org/10.1016/j.compositesa.2006.07.005>.
- Zhang, Y. and Wang, L. (2018), "Thermally stimulated nonlinear vibration of rectangular single-layered black phosphorus", *J. Appl. Phys.*, **124**(13), 10.1063/1.5047584.  
<https://doi.org/10.1063/1.5047584>